ACS Catalysis

Research Article

pubs.acs.org/acscatalysis

Electrodeposition from Acidic Solutions of Nickel Bis(benzenedithiolate) Produces a Hydrogen-Evolving Ni−S Film on Glassy Carbon

Ming Fang,[†] Mark H. Engelhard,[‡] Zihua Zhu,[‡] Monte L. Helm,[†] and John A. S. Roberts*[,†]

[†]Center for Molecular Electrocatalysis, Physical Sciences Division, Pacific Northwest National Laboratory, P.O. Box 999 (K2-57), Richland, Washington 99352, United States

[‡]Environmental Molecular Sciences Laboratory, Pacific Northwest National Laboratory, Richland, Washington 99352, United States

Supporting Information

ABSTRACT: Films electrodeposited onto glassy carbon electrodes from acidic acetonitrile solutions of $[Bu_4N][Ni(bdt)_2]$ (bdt = 1,2-benzenedithiolate) are active toward electrocatalytic hydrogen production at potentials 0.2−0.4 V positive of untreated electrodes. This activity is preserved when the electrode is rinsed and transferred to a fresh acid solution. X-ray photoelectron spectra indicate that the deposited material contains Ni and S, and time-of-flight secondary ion mass spectrometry shows that electrodeposition decomposes the $Ni(bdt)_2$ assembly. Correlations between voltammetric and spectroscopic results indicate that the deposited material is active, i.e., that catalysis is heterogeneous rather than homogeneous. Control experiments establish that obtaining the observed catalytic response requires both Ni and the 1,2-benzenedithiolate ligand to be present during deposition.

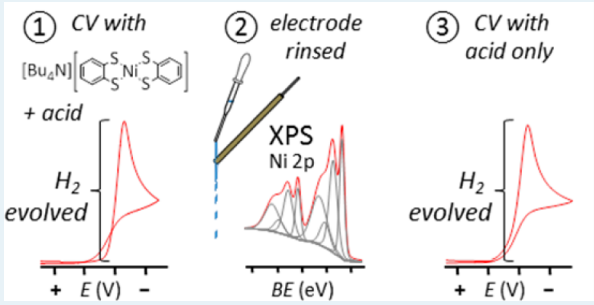

KEYWORDS: *hydrogen, electrocatalysis, electrodeposition, nickel thiolate, electrode modification*

INTRODUCTION

The pursuit of methods for on-demand storage and recovery of electrical energy has emerged as one of the central challenges in energy science. Meeting this challenge could have impacts ranging from grid-level infrastructure to portable devices. Of the different approaches being explored, the use of electrocatalysis to interconvert electrical potential and chemical fuels holds two key advantages: in the energy density of chemical fuels themselves[1] and in the high efficiency with which electrical and chemical energy can in principle be interconverted at low temperatures.[2] The simplest case, the production and oxidation of H_2, has been examined with homogeneous[3] and heterogeneous catalysts,[4] adsorbed and chemisorbed molecular species,[5] and enzymes.[6]

The development of homogeneous electrocatalysts in particular has progressed rapidly because of the precise control over catalyst structure, the uniformity of active sites, and the detailed kinetic and thermodynamic information offered by solution synthetic and spectroscopic methods.[3] However, the understanding of catalyst−electrode interactions in homogeneous electrocatalytic systems is often lacking in detail.[7] Intermediates in multiproton, multielectron electrocatalytic reactions may assume several different protonation and oxidation states, and these intermediates may differ in solubility and stability. Establishing whether adsorption occurs is not trivial,[7,8] and systems in which the spontaneous adsorption of catalytic intermediates can occur are not amenable to the straightforward analyses of catalyst performance that solution voltammetric methods offer.[9]

Herein, we demonstrate electrocatalytic H_2 production with $[Bu_4N][Ni(bdt)_2]$ [tetrabutylammonium bis(1,2-benzenedithiolate)nickel] in acidic MeCN (acetonitrile), arising from the deposition of a film onto a glassy carbon electrode surface. We show that this film is the active catalyst material and present X-ray photoelectron spectroscopic (XPS) evidence showing that this film consists of Ni−S and Ni−O species. These results demonstrate that catalysis at the potentials observed requires both Ni and the 1,2-benzenedithiolate ligand and is in fact heterogeneous. We also present time-of-flight secondary ion mass spectra (ToF-SIMS) collected from the electrodeposited film and from relevant controls. These measurements indicate that the structure of the parent complex is retained when it is deposited onto glassy carbon by evaporation from neutral or acidic MeCN but that this species decomposes upon reductive electrodeposition from an acidic solution. The findings presented here indicate a possible approach to the modification of electrodes for electrocatalytic reactions using molecular precursors and should inform the development of molecular electrocatalysts having similar structures.

Received: August 13, 2013
Revised: October 25, 2013
Published: November 22, 2013

   dx.doi.org/10.1021/cs400675u | ACS Catal. 2014, 4, 90−98

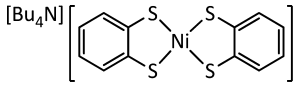

[Bu4N][Ni(bdt)2]

RESULTS

We prepared $[Bu_4N][Ni(bdt)_2]$ using the method of Gray and co-workers.[10] Its cyclic voltammogram (CV) in MeCN [0.2 M $[Bu_4N]PF_6$ (Figure 1, blue trace)] shows a reversible wave with an $E_{1/2}$ of −0.94 V versus $Fc^{+/0}$ (the ferrocenium/ferrocene half-wave potential, used throughout as the reference) corresponding to the $[Ni(bdt)_2]^{-/2-}$ couple. The peak currents vary linearly with $\upsilon^{1/2}$ (Figure S1 of the Supporting Information; υ is the potential scan rate), indicating diffusion control.[11] Adding the acid $[4\text{-}BrC_6H_4NH_3]BF_4$ [4-bromoanilinium tetrafluoroborate (pK_a^{MeCN} = 9.43), 10 mM][12] affords a new stoichiometric reduction wave with a peak potential (E_p) of −0.75 V that shows no accompanying oxidation wave in the return sweep with a υ of 0.1 V s^{-1} (Figure 1, black trace) but becomes quasi-reversible when the scan rate is increased (Figure S2 of the Supporting Information; with υ = 49 V s^{-1}, $E_{1/2}$ = −0.72 V, $i_{p,ox}/i_{p,red}$ = 0.99, and ΔE_p = 145 mV), suggesting a chemical step following the reduction. Scanning to more negative potentials reveals a large irreversible wave with an onset near −1.0 V and an E_p of −1.3 V (Figure 1, red trace), again showing a linear dependence of i_p on $\upsilon^{1/2}$ (Figure S3 of the Supporting Information). Production of H_2 during bulk electrolysis at −1.20 V with $[Bu_4N][Ni(bdt)_2]$ (1 mM) and $[4\text{-}BrC_6H_4NH_3]BF_4$ (30 mM) is confirmed by gas chromatography. Without added Ni complex, the acid is reduced with an onset potential of −1.5 V (Figure 1, green trace).

Voltammograms of $[Bu_4N][Ni(bdt)_2]$ (5–200 μM) with $[4\text{-}BrC_6H_4NH_3]BF_4$ (10 mM; Figure 2A) show an anodic shift in peak potential E_p with an increase in Ni concentration but no increase in peak current i_p, responses that are inconsistent with homogeneous catalysis. Traversing the catalytic wave deposits a film on the electrode surface that is active toward H_2 evolution. This is demonstrated in the two traces shown in Figure 2B. The black trace, obtained in an acidic $[Bu_4N][Ni(bdt)_2]$ solution, shows a single cathodic sweep ending at −1.8 V with no return sweep. The red trace shows a subsequent voltammogram using the same electrode after thorough rinsing with MeCN and transfer to a fresh acid solution without any added $[Bu_4N][Ni(bdt)_2]$. The second scan gives E_p and i_p values similar to those observed in the first scan, indicating a persistent catalytic response. Dissolved $[Ni(bdt)_2]^-$ may also be active for catalysis; however, the current obtained with the electrode after rinsing and transfer to a fresh acid solution is undiminished in magnitude, suggesting that the heterogeneous contribution is dominant.

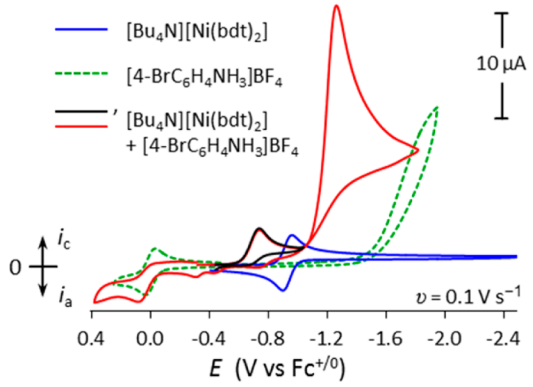

Figure 1. Cyclic voltammograms showing the reduction of $[Bu_4N][Ni(bdt)_2]$ (1 mM) in MeCN (0.2 M $[Bu_4N]PF_6$) before the addition of acid (blue) and after the addition of acid $[4\text{-}BrC_6H_4NH_3]BF_4$ (10 mM), with the switching potential set to −1.1 V (black) or −1.8 V (red), and the reduction of $[4\text{-}BrC_6H_4NH_3]BF_4$ (10 mM) in MeCN (0.2 M $[Bu_4N]PF_6$) without added $[Bu_4N][Ni(bdt)_2]$ (green).

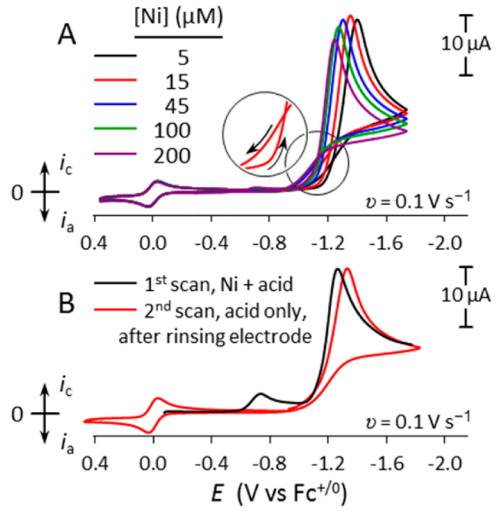

Figure 2. (A) Voltammograms of $[Bu_4N][Ni(bdt)_2]$ (5, 15, 45, 100, and 200 μM) with $[4\text{-}BrC_6H_4NH_3]BF_4$ (10 mM) in MeCN (0.2 M $[Bu_4N]PF_6$; 1 mm glassy carbon electrode) showing catalytic H_2 production. (B) Linear sweep voltammogram of $[Bu_4N][Ni(bdt)_2]$ (1 mM) with $[4\text{-}BrC_6H_4NH_3]BF_4$ (10 mM) in MeCN (0.2 M $[Bu_4N]PF_6$; black) and a subsequent CV using the same electrode after rinsing and transfer to fresh $[4\text{-}BrC_6H_4NH_3]BF_4$ (10 mM) in MeCN (0.2 M $[Bu_4N]PF_6$) without added Ni complex (red).

Applying a 3 min cathodic potential step with the electrode in an acidic $[Bu_4N][Ni(bdt)_2]$ solution reproducibly generates a catalytically active film. Varying the applied potential [−1.4, −1.9, and −2.4 V (Figure 3)] changes the response observed with the electrode when it is transferred to a fresh $[4\text{-}BrC_6H_4NH_3]BF_4$ solution after rinsing. Values of E_p and i_p

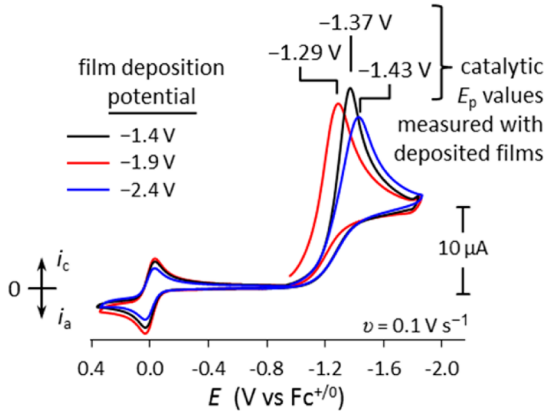

Figure 3. Voltammograms of $[4\text{-}BrC_6H_4NH_3]BF_4$ (10 mM) in MeCN (0.2 M $[Bu_4N]PF_6$) using electrodes prepared by a 3 min potential step electrodeposition from $[Bu_4N][Ni(bdt)_2]$ (1.0 mM) with $[4\text{-}BrC_6H_4NH_3]BF_4$ (10 mM) in MeCN (0.2 M $[Bu_4N]PF_6$) followed by rinsing. Potentials used in the electrodeposition are given in the legend, and peak potentials in the subsequent catalytic experiments are shown above the corresponding peaks.

dx.doi.org/10.1021/cs400675u | ACS Catal. 2014, 4, 90−98

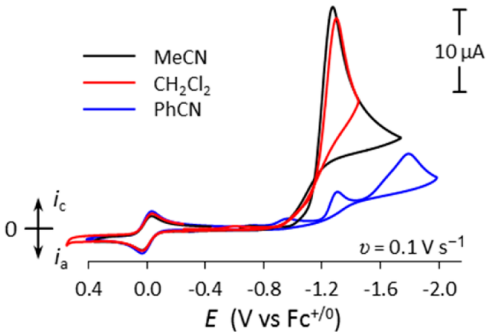

Figure 4. Cyclic voltammograms of $[Bu_4N][Ni(bdt)_2]$ (0.1 mM) and $[4\text{-}BrC_6H_4NH_3]BF_4$ (10 mM) in 0.2 M $[Bu_4N]PF_6$ solutions with solvents MeCN, CH_2Cl_2, and PhCN.

depend on the potential applied in the deposition step in a nonlinear fashion, showing that the formation of the catalytically active film is highly sensitive to the deposition conditions. Because the potential applied during film formation influences the catalytic properties of the film, deposition must involve one or more reduction steps. Some deposition from the acidic $[Bu_4N][Ni(bdt)_2]$ solution is observed even without applying a reducing potential during the deposition; however, the peak potential observed after rinsing and transfer to fresh acid is more negative [E_p = −1.46 V (Figure S4 of the Supporting Information)].

Controls using either $Na_2(bdt)$ or $[Ni(MeCN)_6](BF_4)_2$ rather than the $[Bu_4N][Ni(bdt)_2]$ complex were conducted to evaluate the origin of the catalytic response. Both render the electrode active toward H_2 evolution, but at potentials considerably more negative than that observed with the $[Ni(bdt)_2]^-$ complex. Voltammetry of $Na_2(bdt)$ (0.5 mM, with 2 equiv of 15-crown-5 added) and $[4\text{-}BrC_6H_4NH_3]BF_4$ (10 mM) in MeCN affords a catalytic wave with an E_p of −1.70 V (Figure S5 of the Supporting Information). Voltammetry of $[Ni(MeCN)_6](BF_4)_2$ with $[4\text{-}BrC_6H_4NH_3]BF_4$ in MeCN without the bdt ligand affords a catalytic current having an E_p of −1.48 V with 1 mM Ni and an E_p of −1.67 V with 0.1 mM Ni (Figure S6 of the Supporting Information). These CVs show irreversible oxidation waves with E_p values from −0.35 to −0.15 V assigned to anodic stripping of Ni metal. An irreversible wave in this potential window is also seen with acidic $[Ni(bdt)_2]^-$ solutions (Figure 1, red trace) but is much smaller than that with $[Ni(MeCN)_6](BF_4)_2$. This feature is not observed in CVs recorded after film deposition from acidic $[Ni(bdt)_2]^-$ and transfer to fresh acid.

To examine the role of solvent polarity and aromaticity, the CVs of $[Bu_4N][Ni(bdt)_2]$ with $[4\text{-}BrC_6H_4NH_3]BF_4$ in CH_2Cl_2 and PhCN (benzonitrile) as solvents were compared with CVs in MeCN (Figure 4). MeCN and CH_2Cl_2 afford nearly superimposable traces; however, PhCN gives a completely different response, suggesting solvent aromaticity plays a role in film formation. This is examined in detail below. CVs of $[Bu_4N][Ni(bdt)_2]$ in MeCN with different $[4\text{-}BrC_6H_4NH_3]BF_4$ concentrations (Figure S7 of the Supporting Information) and with other acids (Figure S8 of the Supporting Information) are included.

The effect of electrodeposition on the $[Ni(bdt)_2]^-$ moiety was examined by ToF-SIMS measurement of a glassy carbon plate sample prepared by electrodeposition from a solution of $[Bu_4N][Ni(bdt)_2]$ in acidic MeCN using a 3 min potential step to −1.9 V as described above. The positive and negative ion spectra from this sample were compared to those of samples prepared by evaporating the solvent from droplets of $[Bu_4N][Ni(bdt)_2]$ dissolved in either acidic or neutral MeCN (drop-casting) and to those of an unmodified glassy carbon plate (the blank). Mass spectrometric data indicating the presence or absence of S, Ni, the bdt ligand and fragments obtained by protonation or by removal of S, and the parent $Ni(bdt)_2$ species along with the Ni(bdt) fragment are presented for these four samples in Table S1 of the Supporting Information. Selected portions of the mass spectra are presented in Figures 5 and 6, and the complete set of mass spectra accompanying the entries in Table S1 is presented in Figures S9−S15 of the Supporting Information.

The primary findings are as follows. Electrodeposition incorporates Ni at greater abundances than in the control samples. The $Ni(bdt)_2$ species remains intact on drop-casting from either an acidic or a neutral solution but decomposes upon electrodeposition. Signals for ^{32}S were identified in all of the mass spectra; however, fragments corresponding to Ni_xS_y species were not observed. These data are therefore inconclusive with regard to the formation of nickel sulfides.

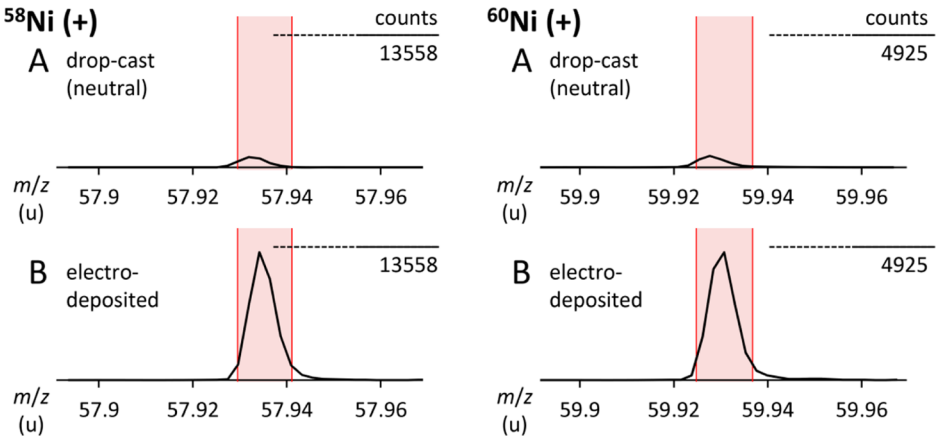

Figure 5. Positive ion mass spectra of glassy carbon plates (A) with $[Bu_4N][Ni(bdt)_2]$ drop-cast from neutral MeCN and (B) modified by immersion in $[Bu_4N][Ni(bdt)_2]$ (1.0 mM) with $[4\text{-}BrC_6H_4NH_3]BF_4$ (10 mM) in MeCN (0.2 M $[Bu_4N]PF_6$) with a 3 min potential step to −1.9 V vs $Fc^{+/0}$. Regions correspond to the expected m/z range for the species listed above each set of spectra. Pink bars are centered on the exact mass of the most abundant isotopomers and span a range of 0.01% of that exact mass.

dx.doi.org/10.1021/cs400675u | ACS Catal. 2014, 4, 90−98

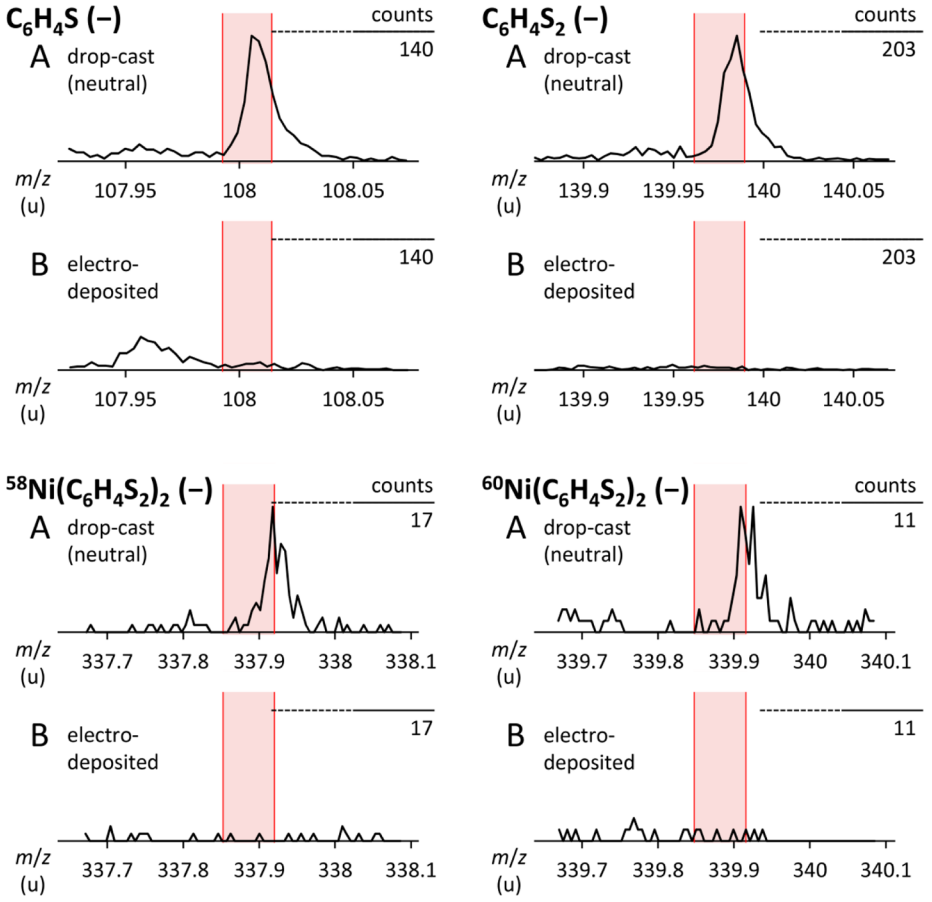

Figure 6. Negative ion mass spectra of glassy carbon plates (A) with $[Bu_4N][Ni(bdt)_2]$ drop-cast from neutral MeCN and (B) modified by immersion in $[Bu_4N][Ni(bdt)_2]$ (1.0 mM) with $[4\text{-}BrC_6H_4NH_3]BF_4$ (10 mM) in MeCN (0.2 M $[Bu_4N]PF_6$) with a 3 min potential step to −1.9 V vs $Fc^{+/0}$. Regions correspond to the expected *m*/*z* range for the species listed above each set of spectra. Pink bars are centered on the exact mass of the most abundant isotopomers and span a range of 0.01% of that exact mass.

Lines corresponding to $^{58}Ni^+$ and $^{60}Ni^+$ in their characteristic ratio of 2.6:1 are evident in the positive ion spectra for both the electrodeposited and drop-cast samples; however, the signal from the electrodeposited material is larger than for the neutral or acidic drop-cast samples, by factors of 14 and 17, respectively (Table S1, entries 2 and 3, Figure 5, and Figure S10 of the Supporting Information). Signals for $^{58}Ni^1H^+$ and $^{60}Ni^1H^+$ are seen in the electrodeposited sample but not the drop-cast samples, suggesting that Ni−H bond formation is triggered by reduction (Table S1, entries 4 and 5, and Figure S11 of the Supporting Information).

Mass spectra showing the parent $Ni(bdt)_2$ ions and selected fragments are given in Figure 6. The $Ni(bdt)_2$ species and the Ni(bdt) fragment are both observed in the drop-cast samples (Table S1, entries 9−12, and Figures S14 and S15 of the Supporting Information), as are peaks corresponding to $C_6H_4S_2$ and $C_6H_5S_2$ (Table S1, entries 7 and 8, and Figures S12 and S13 of the Supporting Information). A peak assigned to the most abundant isotopomer of C_6H_4S also appears in the negative ion spectrum of the sample drop-cast from a neutral solution (Table S1, entry 6, and Figure S13 of the Supporting Information). These data show that neither the parent ions nor any of the fragments mentioned above are detected in the electrodeposited material, indicating that the bdt ligand is either lost to solution or consumed during electrodeposition. This is addressed in more detail in the Discussion.

The film composition was examined by XPS, again using glassy carbon plate samples. These were prepared by immersion in an acidic $[Ni(bdt)_2]^-$ solution either with or without a potential step to −1.9 V, followed by thorough rinsing with MeCN (Figures S16−S22 of the Supporting Information). The potential-stepped and immersed samples both show deposited Ni and S by XPS; however, these signals are much larger with the potential-stepped sample (Figure 7). Disk electrodes prepared in precisely the same way were examined by CV (Figure S4 of the Supporting Information). The results of these parallel voltammetric measurements are consistent with the primary finding that cathodic electrodeposition generates a catalytically active Ni−S film. XPS peak assignments and a quantitative line fitting analysis are presented in the Discussion. Variation in the Ni 2p signal intensities and line shapes from the two areas measured with the potential-stepped sample indicates heterogeneity in the distribution of deposited material. The lines at 853.3, 856.3, and 870.8 eV are proportionately larger in the area having more abundant Ni. Areas not exposed to the $[Ni(bdt)_2]^-$ solution exhibited F, C, O, Si, and a trace of S, but no Ni (Figures S18 and S20 of the Supporting Information).

DISCUSSION

This contribution describes electrocatalytic H_2 production with a well-known bis(dithiolate) complex of Ni and, more specifically, heterogeneous catalysis arising from this species,

dx.doi.org/10.1021/cs400675u | ACS Catal. 2014, 4, 90−98

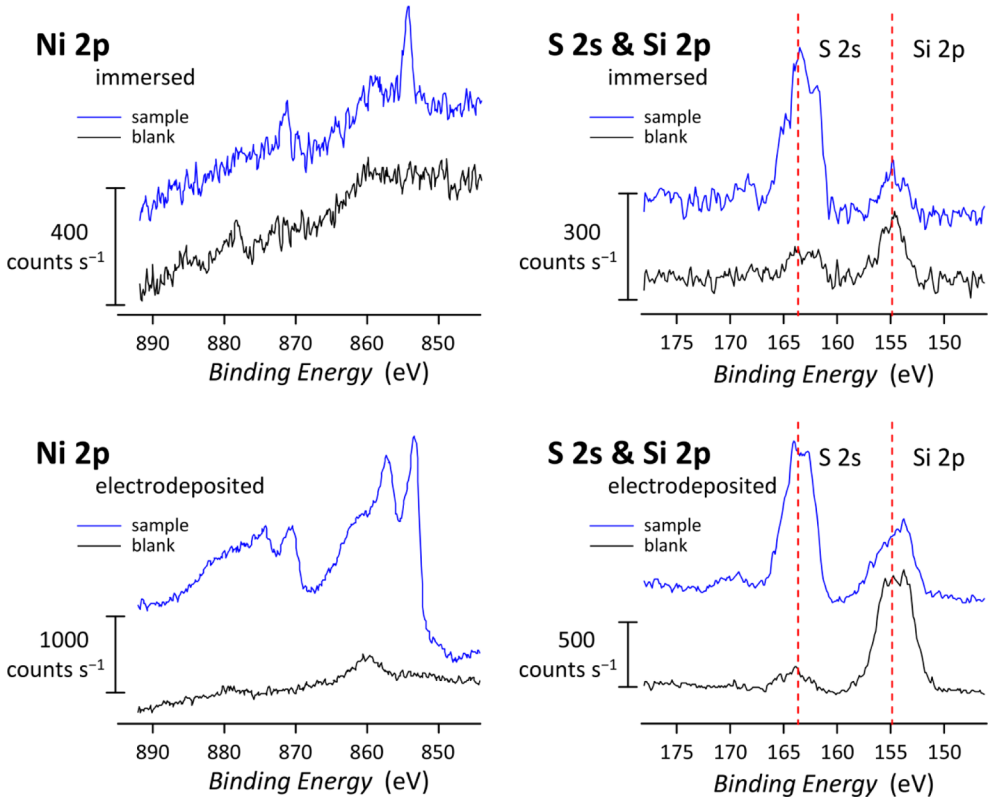

Figure 7. High-resolution photoemission spectra of glassy carbon plates (blue, obtained from a portion modified as described below; black, obtained from an unmodified portion of the same sample). Samples were immersed in $[Bu_4N][Ni(bdt)_2]$ (1.0 mM) in MeCN and subsequently rinsed (A) or immersed in $[Bu_4N][Ni(bdt)_2]$ (1.0 mM) with $[4\text{-}BrC_6H_4NH_3]BF_4$ (10 mM) in MeCN (0.2 M $[Bu_4N]PF_6$), subjected to a 3 min potential step to −1.9 V vs $Fc^{+/0}$, and then rinsed (B). Regions correspond to the expected range of binding energies denoted by the element and orbital listed above each set of spectra.

which appears to operate as a precursor to a heterogeneous catalyst material. The challenge of attributing catalysis to a particular dissolved species or to a new soluble or insoluble material generated from it under catalytic conditions[8] is particularly important in the context of electrode reactions,[13] because these reactions are inherently heterogeneous. Both H_2 production and electrodeposition are known for metal dithiolene complexes. Electrodeposition has been developed as a route to optoelectronic devices; for example, molecular Cu and Ni dithiolene complexes have been electrodeposited anodically onto Pt, indium tin oxide, and fluorine-doped tin oxide.[14] A substantial number of transition metal dithiolate complexes evolve H_2, and research in this area continues to produce valuable insights into synthetic and natural catalyst systems. In 1991, Moll and co-workers reported the stoichiometric evolution of H_2 by reacting $[Fe(bdt)_2]^{2-}$ with HCl. A variety of catalytic H_2 production systems involving metal dithiolenes have since emerged. $[Bu_4N][Co(bdt)_2]$ is an active photo- and electrocatalyst for H_2 evolution;[15] Eisenberg, Holland, and co-workers have reported photocatalytic H_2 production with Ni tris(pyridine-2-thiolate),[16] and with *in situ*-generated Ni dithiolate complexes arising in an aqueous system consisting of CdSe nanocrystals, dihydrolipoic acid, and Ni(II).[17] In a recent example very closely related to the system discussed herein, monoanionic Ni bis(1,2-ethylenedithiolate-1,2-dimethyl ester) was reported as a precursor to heterogeneous H_2 production electrocatalysis with 4-toluenesulfonic acid in MeCN;[18] however, this result was found by others to be irreproducible.[15] Bimetallic systems featuring M−S bonds have been developed as models for the hydrogenase enzymes, and some of these are active catalysts. Gloaguen and co-workers demonstrated electrocatalytic H_2 production with the FeFe hydrogenase model $Fe_2(\mu\text{-bdt})(CO)_6$,[19] and Chiang and co-workers have recently described the related diiron complex $[Fe_2(\mu\text{-bdt})(\mu\text{-}PPh_2)(CO)_5]^-$ and its singly and doubly protonated forms, showing that the S atoms of bdt may act as proton relays during catalysis;[20] several heterobimetallic Ni−Fe hydrogenase mimics with Ni−S bonds developed by Rauchfuss and co-workers show exceptional activity as electrocatalysts for H_2 production.[21]

With a glassy carbon electrode prepared by conventional polishing methods immersed in a MeCN solution of $[Bu_4N][Ni(bdt)_2]$ and $[4\text{-}BrC_6H_4NH_3]BF_4$, we have observed that applying a cathodic potential sweep or potential step modifies the electrode such that catalytic activity is retained on rinsing and transfer to a fresh solution containing the catalytic substrate. In parallel CV, ToF-SIMS, and XPS measurements, we have determined that Ni and S are deposited cathodically and that the deposited material produces the observed catalytic response. In the following paragraphs, we develop additional lines of reasoning that support this conclusion.

The voltammetric data exhibit time-dependent features consistent with an induction period during which active material is formed from inactive or mildly active precursors. In CVs of $[Bu_4N][Ni(bdt)_2]$ with $[4\text{-}BrC_6H_4NH_3]BF_4$ in MeCN (Figure 2A, inset), the current at −1.1 V is larger in the return sweep than in the initial cathodic sweep, indicating that the catalytic activity is higher when this potential is revisited,

dx.doi.org/10.1021/cs400675u | *ACS Catal.* 2014, 4, 90−98

i.e., that the activity has increased as a function of time. This suggests an induction period during which the active material is formed, one of Finke's "telltale signs" of heterogeneous catalysis from soluble catalyst precursors.[8] After samples had been rinsed and transferred to a fresh acid solution, the crossing observed in the initial scan with dissolved $[Ni(bdt)_2]^-$ present (Figure 2A, inset) is no longer seen (Figure 2B, red trace), indicating that once activated, the electrode remains so. These observations constitute further evidence of heterogeneous catalysis.[7]

Solvent polarity has little apparent effect: the voltammograms of $[Bu_4N][Ni(bdt)_2]$ in acidic MeCN (dielectric constant ε = 37.5) and CH_2Cl_2 (ε = 8.93) are nearly superimposable (Figure 4). The aromatic solvent PhCN (ε = 26.0), however, gives a completely different response, suggesting $\pi-\pi$ interactions that involve the 1,2-benzenedithiolate ligands and are disrupted by this solvent in particular.[22] Interaction between $Ni(bdt)_2$ moieties and $[4\text{-}BrC_6H_4NH_3]^+$ molecules, also aromatic, do not appear to be needed for catalysis: the nonaromatic substrate dimethylformamide·triflic acid affords a similar catalytic response (Figure S8 of the Supporting Information). Intermolecular $\pi-\pi$ interactions among $Ni(bdt)_2$ moieties in a hypothetical bimetallic catalytic pathway could be influenced by solvent aromaticity, but the dependence of the catalytic peak current on concentration observed in MeCN is inconsistent with a putative bimetallic homogeneous catalytic route (Figure 2A). Alternately, the operative $\pi-\pi$ interactions may involve arene structures at the glassy carbon surface itself.[23] Adsorption of metal complexes with aromatic ligands onto glassy carbon has been known for some time.[24] If these interactions are required in this case for the formation of the active material, their disruption would certainly interfere with catalysis.

Decomposition of $Ni(bdt)_n$ moieties at the surface may also be important: Hydrodesulfurization of petroleum feedstocks using heterogeneous Ni-containing catalysts offers a compelling chemical rationale for considering cleavage of the C−S bond in the bdt ligand.[25] The involvement of Ni(I) species in enzyme-mediated C−S bond cleavage has also been hypothesized.[26] Thus, while the solvent dependence data suggest that $\pi-\pi$ interactions may be involved in the initial steps of formation of the catalytically active material, it is possible that the original $Ni(bdt)_2$ coordination complex does not persist during catalysis. This question motivated the comparison of mass spectra from electrodeposited films with those obtained from films prepared by simple evaporation. Signals for the parent $Ni(bdt)_2$ moiety and several characteristic fragments were observed with the films prepared by evaporation, but none of these were present in the electrodeposited sample, suggesting that the parent structure is indeed decomposed during electrodeposition. Both Ni and S were, however, observed in the electrodeposited material.

XPS also reveals the deposition of both Ni and S atoms on the glassy carbon surface during electrodeposition. The high-resolution Ni 2p photoemission spectrum (Figure 8 and S21 of the Supporting Information, red traces) is similar to a spectrum reported with a single-layer sample of the two-dimensional coordination polymer $[Ni_3(benzenehexathiolate)_2]$ on highly oriented pyrolitic graphite (these spectra are dominated by the Ni−S interactions).[27] The features at 853.3 and 870.8 eV are also observed with electrodeposited layered Ni−S thin films[28] and with sulfided Ni on $MgSiO_3$.[29] The line at 856.8 eV is consistent with NiO or $Ni(OH)_2$.[30] A peak-fitting analysis of the Ni 2p region based on these assignments (Figure 8) affords estimates of 0.7 and 0.8 atom % for Ni in the Ni−O and Ni−S

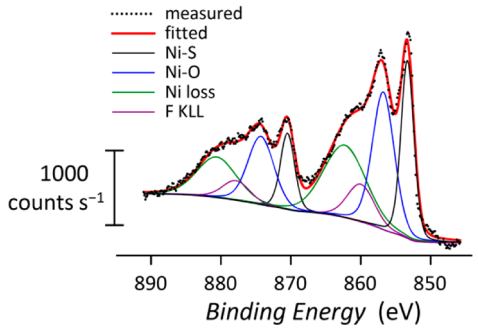

Figure 8. High-resolution photoemission spectrum (Ni 2p) of a glassy carbon plate immersed in $[Bu_4N][Ni(bdt)_2]$ (1.0 mM) with $[4\text{-}BrC_6H_4NH_3]BF_4$ (10 mM) in MeCN (0.2 M $[Bu_4N]PF_6$) and subjected to a 3 min potential step to −1.9 V vs $Fc^{+/0}$. Peak fitting with Ni oxide/hydroxide and Ni sulfide lines and F Auger lines as described in the Supporting Information.

environments, respectively. This fitting includes contributions from the F KL_1L_1 and KL_1L_{23} Auger lines. Details are given in Figure S21 and Table S1 of the Supporting Information.

The line observed at 853.3 eV may have a contribution from Ni metal (852.6 eV).[31] However, the loss lines at 856.3 and 858.0 eV observed with Ni metal are weak and do not by themselves account for the higher-energy $2p_{1/2}$ signals observed in this case. This does not rule out the presence of Ni metal in the sample, its generation under catalytic conditions, or its relevance as a possible H_2 production electrocatalyst.[32] The S 2p signal at 163.6 eV is consistent with Ni_xS_y phases;[29,33] however, some intensity in this region is also observed in the background spectra (Figure S21 of the Supporting Information). Quantitative analysis based on the deconvolution described above affords a Ni:S ratio of 0.9:1 (Tables S2 and S3 of the Supporting Information), suggesting a NiS phase has formed. The alternate interpretation, that the Ni is present as Ni(0) and the S is noninteracting, is counterintuitive given that the thiophilicity of Ni drives much of its bioinorganic chemistry.[34] Our control experiments and results reported by other groups also lend support to the hypothesis that NiS is formed. Reduction of $[Ni(MeCN)_6]^{2+}$ in an acidic solution does afford a catalytic response (Figure S6 of the Supporting Information); however, catalysis in this case is initiated at more negative potentials, and much higher Ni concentrations are required. Both Ni_xS_y (x = 3 and y = 2; x = 7 and y = 6; x = 1 and y = 1) phases and metallic Ni are reported to evolve H_2.[28] Howover, the Ni−S materials have been shown to evolve H_2 at more moderate potentials than Ni metal under identical conditions, with the best performance observed using α-NiS.[35]

Measurements by XPS also revealed small amounts of codeposited Na, Zn, Co, and Ca (Figure S17 of the Supporting Information), likely reflecting the range of metals, coordination geometries, and oxidation states that the 1,2-benzenedithiolate ligand is capable of supporting.[36] Arene-1,2-dithiolates have, for example, been used for quantitative demetalation of other ligands, as with CuCl complexes in the recovery of expensive chiral diphosphines.[37] However, the control experiments described above with $[(15\text{-crown-5})Na]_2(bdt)$ added instead of $[Bu_4N][Ni(bdt)_2]$ showed catalysis only at fairly negative potentials (Figure S5 of the Supporting Information), demonstrating that the Ni complex is required for catalysis at moderate potentials. The collected XPS and voltammetric evidence, along with results already reported, supports our

dx.doi.org/10.1021/cs400675u | ACS Catal. 2014, 4, 90−98

attribution of catalysis to the presence of Ni−S species on the electrode.

CONCLUSIONS

Under the conditions employed in this study, $[Ni(bdt)_2]^-$ is a precursor to electrode-bound Ni−S species showing remarkable activity toward electrocatalytic H_2 evolution. Differentiating between homogeneous and heterogeneous electrocatalysis when beginning with a dissolved precursor or catalyst is not trivial in general;[7,8] however, it is sometimes easier to demonstrate heterogeneous electrocatalysis than it is to rule it out, as the present case illustrates. Notwithstanding these challenges, the promise for significant catalytic performance is readily apparent in the large catalytic currents already observed. Electrosynthetic routes to well-defined surface metal sulfide cluster structures on chemically inert substrates may aid in the understanding of important heterogeneous catalyst systems and the discovery of new ones, particularly for electrocatalytic transformations of small molecules such as H_2, O_2, N_2, and H_2O.

EXPERIMENTAL SECTION

Materials and Methods. Schlenk techniques or a N_2 atmosphere glovebox were used for all manipulations. Acetonitrile (MeCN; Alfa-Aesar, anhydrous, amine-free), dichloromethane (CH_2Cl_2; Fisher, not stabilized), and diethyl ether (Et_2O; VWR, not stabilized) were purified by being sparged with nitrogen and passed through neutral alumina using a solvent purification system (PureSolv, Innovative Technologies, Inc.). Acetone (reagent; Fisher) and ethylene glycol (anhydrous; Aldrich) were used as received. Tetrabutylammonium hexafluorophosphate ($[Bu_4N]PF_6$) was prepared from $[Bu_4N]I$ and $[NH_4]PF_6$ (Aldrich) and purified by crystallization from a saturated acetone solution.[38] Ferrocene (Fc; Aldrich) was purified by sublimation. Tetrafluoroboric acid etherate ($HBF_4{\cdot}Et_2O$; Aldrich) was used as received and stored at −35 °C in the glovebox. Disodium benzenedithiolate [Na_2(bdt)], 1,4,7,10,13-pentaoxacyclopentadecane (15-crown-5), 4-bromoaniline (4-$BrC_6H_4NH_2$), 4-anisidine (4-$MeOC_6H_4NH_2$), and 2,4,6-collidine (2,4,6-$Me_3C_5H_2N$) were used as received (Aldrich). $[4\text{-}BrC_6H_4NH_3]BF_4$, $[4\text{-}MeOC_6H_4NH_3]BF_4$, and $[2,4,6\text{-}Me_3C_5H_2NH]BF_4$ were synthesized by slow addition of $HBF_4{\cdot}Et_2O$ to an Et_2O solution of ∼5% excess base. The precipitate was collected by filtration, washed with excess Et_2O, and recrystallized from a MeCN/Et_2O mixture in a glovebox. $[Ni(MeCN)_6](BF_4)_2$ was prepared following a reported procedure.[39] Stock solutions were prepared as needed using volumetric glassware and gastight syringes in the glovebox and were used immediately. Solid and liquid solutes were quantitated by mass.

Instrumentation and Analytical Methods. *Voltammetric Measurements.* These were conducted using a CH Instruments 620D potentiostat and a standard three-electrode cell. All electrochemical measurements and electrode manipulations were conducted in a N_2 glovebox. Unless otherwise noted, the working electrode was a 1 mm glassy carbon disk encased in polyether−ether−ketone (PEEK; ALS), cleaned using a polishing pad (Buehler MicroCloth) loaded with diamond paste (Buehler MetaDi II 0.25 μm), and lubricated with ethylene glycol and then rinsed with MeCN. A fresh portion of the polishing pad was used for each polishing operation. The counter electrode was a 3 mm diameter glassy carbon rod (Alfa Aesar). The reference electrode was a silver wire (Alfa Aesar, 1 mm diameter, 99.9%) anodized for 5 min in aqueous HCl (Aldrich), washed with water and acetone, dried, and suspended in a glass tube containing neutral MeCN (0.2 M $[Bu_4N]PF_6$) and fitted with a porous Vycor disk.

Bulk Electrolyses. These were conducted using a BASi EC epsilon potentiostat equipped with a PWR-3 high-power/current module. The cell was a 45 mL glass vial equipped with a plastic cap, a reticulated vitreous carbon working electrode (half-cylinder, 10 mm diameter, 30 mm length), a reference electrode (1 mm AgCl-coated Ag wire in a 2 mm perfluorinated ethylene propylene tube with a Vycor tip), a counterelectrode (coiled 0.25 mm Nichrome wire in a 6.5 mm glass tube with a Vycor tip), and a stir bar. This cell was calibrated for volume and found to hold 35 mL. Gas analysis for H_2 evolved during bulk electrolysis was performed using an Agilent 6850 gas chromatograph fitted with a 10 ft Supelco 1/8″ Carbosieve 100/120 column, calibrated with two $H_2/N_2/Ar$ gas mixtures of known composition.

X-ray Photoelectron Spectroscopic (XPS) Measurements. XPS samples were prepared using 4 mm × 10 mm × 10 mm glassy carbon plates (SPI-Glas 22 grade, SPI supplies) polished as described above. These samples were received and mounted for XPS analysis inside a N_2-purged recirculated glovebox (<0.2 ppm O_2, H_2O dew point of −80 °C) on a standard 75 mm × 75 mm sample holder (Physical Electronics) using stainless steel screws. The sample holder was then placed into the XPS vacuum introduction system and pumped to $<1 \times 10^{-7}$ mmHg using a turbomolecular pumping system prior to introduction into the main ultra-high-vacuum system. The main vacuum system pressure is maintained at 1×10^{-10} mmHg during analysis and pumped using a series of sputter ion pumps and turbo-molecular pumps. Measurements were performed with a Physical Electronics Quantera Scanning X-ray Microprobe. This system uses a focused monochromatic Al Kα X-ray (1486.7 eV) source for excitation and a spherical section analyzer. The instrument has a 32-element multichannel detection system. A 100 W X-ray beam focused to a 100 μm diameter was rastered over a 1.3 mm × 1 mm rectangle on the sample. The X-ray beam is incident normal to the sample, and the photoelectron detector is at 45° off-normal. High-energy resolution spectra were collected using a pass energy of 69.0 eV with a step size of 0.125 eV. For the Ag $3d_{5/2}$ line, these conditions produced a full width at half-maximum of 0.91 eV.

Time-of-Flight Secondary Ion Mass Spectrometry (ToF-SIMS). Mass spectra were acquired using a TOF.SIMS 5 spectrometer (IONTOF GmbH, Münster, Germany) with a 25 keV Bi^+ beam. The analysis chamber was maintained at 5.0×10^{-9} mbar during analysis. Glassy carbon plate (4 mm × 10 mm × 10 mm) samples were prepared as described above. The drop-cast samples were prepared by applying MeCN solutions of either $[Bu_4N][Ni(bdt)_2]$ (1 mM) or $[Bu_4N][Ni(bdt)_2]$ (1 mM) and $[4\text{-}BrC_6H_4NH_3]BF_4$ (10 mM) on the clean glassy carbon plates and allowing the solvent to evaporate inside the glovebox. The electrodeposition procedure is detailed below.

Preparation and Characterization of $[Bu_4N][Ni(bdt)_2]$. $[Bu_4N][Ni(bdt)_2]$ was prepared following a reported procedure.[10] Green, crystalline material was obtained by crystallization from a CH_2Cl_2/ether mixture inside the glovebox and recovered by filtration. A single crystal sample was obtained from this batch by diffusing Et_2O into a concentrated CH_2Cl_2 solution. A 10× objective lens microscope was used to identify a suitable crystal for diffractometry, which was coated in

dx.doi.org/10.1021/cs400675u | ACS Catal. 2014, 4, 90−98

Paratone, affixed to a nylon loop, and placed under streaming nitrogen (110 K) in a Bruker KAPPA APEX II CCD diffractometer with 0.71073 Å Mo Kα radiation. The unit cell dimensions were as follows: a = 16.437 Å, b = 19.678 Å, c = 18.558 Å, and $\alpha = \beta = \gamma = 90°$. Previously reported[40] lengths and angles were as follows: a = 16.483 Å, b = 19.715 Å, c = 18.613 Å, $\alpha = \beta = \gamma = 90°$ (for data collected at 220 K). Measured cell lengths are 99.7−99.8% of the reported values, reflecting a dependence of the density of the material on temperature.

Voltammetry of $[Bu_4N][Ni(bdt)_2]$ in Neutral and Acidic Solutions. A typical procedure is illustrated here. A 10 mM Ni stock solution was prepared by diluting $[Bu_4N][Ni(bdt)_2]$ (5.8 mg, 0.010 mmol) to 1.0 mL with MeCN. A 0.50 M acid stock solution was prepared by diluting $[4\text{-}BrC_6H_4NH_3]BF_4$ (129.9 mg, 0.50 mmol) to 1.0 mL with MeCN. A 0.20 M electrolyte stock solution was prepared by diluting $[Bu_4N]PF_6$ (774.9 mg, 2.0 mmol) to 10 mL with MeCN. Cyclic voltammograms were recorded following (1) addition of 0.90 mL of an electrolyte stock solution, (2) addition of 0.10 mL of a $[Bu_4N][Ni(bdt)_2]$ stock solution, and (3) addition of 20 μL of an acid stock solution and ferrocene (one crystal, <0.5 mg). The resultant solution was 1 mM in $[Bu_4N][Ni(bdt)_2]$ and 10 mM in acid.

Electrodeposition of Catalytic Films onto Glassy Carbon from Acidic Solutions of $[Bu_4N][Ni(bdt)_2]$ in MeCN. Typical sample preparation procedures are illustrated here. A solution of $[Bu_4N][Ni(bdt)_2]$ (1 mM), $[4\text{-}BrC_6H_4NH_3]BF_4$ (10 mM), and $[Bu_4N]PF_6$ (0.18 M) prepared as described above and a single crystal of ferrocene (<5 mg) were added to an electrochemical cell.

A. Potential Sweep Electrodeposition. A linear sweep voltammogram (0 V → −1.7 V vs $Fc^{+/0}$; υ = 0.1 V s^{-1}) was recorded using a freshly glassy carbon disk electrode. The electrode was then rinsed by pipet with MeCN (2 × 1.5 mL) and allowed to dry.

B. Potential Step Electrodeposition. A constant potential (e.g., −1.9 V vs $Fc^{+/0}$) was applied for 3 min, using electrodes prepared as described for procedure A, followed by the same rinsing procedure.

C. Sample Preparation for XPS and ToF-SIMS Measurements by Potential Step Electrodeposition Using Glassy Carbon Plates. Procedure B was used with a 4 mm × 10 mm × 10 mm plate as the working electrode, partially immersed in the electrolyte solution and connected to the potentiostat lead by an alligator clip clamped above the liquid level.

Voltammetry of Modified Electrodes in Acidic Solutions. A $[Bu_4N]PF_6$ stock solution (1.0 mL, 0.20 M), 20 μL of a $[4\text{-}BrC_6H_4NH_3]BF_4$ stock solution (0.50 M), and a single crystal (<5 mg) of ferrocene were added to an electrochemical cell. A glassy carbon disk electrode prepared by procedure A or B was introduced as the working electrode, and cyclic voltammograms were recorded.

Bulk Electrolysis. Electrocatalytic H_2 production was confirmed by bulk electrolysis of a MeCN solution of $[Bu_4N][Ni(bdt)_2]$ (1 mM), $[4\text{-}BrC_6H_4NH_3]BF_4$ (30 mM), and $[Bu_4N]PF_6$ (0.2 M) at −1.2 V versus $Fc^{+/0}$, in a bulk electrolysis cell charged with 10 mL of an analyte solution. Samples of the headspace gas were removed via a gastight syringe during the experiment and were analyzed by gas chromatography using detector response calibration to quantify H_2; 9.67 C of charge was passed over 9 min, generating 23 μmol of H_2, corresponding to a 46% Faradaic efficiency.

■ ASSOCIATED CONTENT

Supporting Information

Electrochemical data, mass spectra, and X-ray photoemission spectra. This material is available free of charge via the Internet at http://pubs.acs.org.

■ AUTHOR INFORMATION

Corresponding Author

*E-mail: john.roberts@pnnl.gov.

Notes

The authors declare no competing financial interest.

■ ACKNOWLEDGMENTS

This research was supported as part of the Center for Molecular Electrocatalysis, an Energy Frontier Research Center funded by the U.S. Department of Energy, Office of Science, Office of Basic Energy Sciences. Pacific Northwest National Laboratory is operated by Battelle for the U.S. Department of Energy. A portion of the research was performed using EMSL, a national scientific user facility sponsored by the Department of Energy's Office of Biological and Environmental Research and located at Pacific Northwest National Laboratory. J.A.S.R. thanks Dr. Tianbiao Liu for determination of the unit cell for a single-crystal sample of $[Bu_4N][Ni(bdt)_2]$.

■ REFERENCES

(1) Thackeray, M. M.; Wolverton, C.; Isaacs, E. D. *Energy Environ. Sci.* **2012**, *5*, 7854−7863.
(2) Liang, Y.; Li, Y.; Wang, H.; Dai, H. *J. Am. Chem. Soc.* **2013**, *135*, 2013−2036.
(3) Yang, J. Y.; Bullock, R. M.; DuBois, M. R.; DuBois, D. L. *MRS Bull.* **2011**, *36*, 39−47.
(4) Chen, W.-F.; Sasaki, K.; Ma, C.; Frenkel, A. I.; Marinkovic, N.; Muckerman, J. T.; Zhu, Y.; Adzic, R. R. *Angew. Chem., Int. Ed.* **2012**, *51*, 6131−6135.
(5) Tran, P. D.; Artero, V.; Fontecave, M. *Energy Environ. Sci.* **2010**, *3*, 727−747.
(6) Armstrong, F. A.; Belsey, N. A.; Cracknell, J. A.; Goldet, G.; Parkin, A.; Reisner, E.; Vincent, K. A.; Wait, A. F. *Chem. Soc. Rev.* **2009**, *38*, 36−51.
(7) Artero, V.; Fontecave, M. *Chem. Soc. Rev.* **2013**, *42*, 2338−2356.
(8) Widegren, J. A.; Finke, R. G. *J. Mol. Catal. A: Chem.* **2003**, *198*, 317−341.
(9) Savéant, J. M. *Elements of molecular and biomolecular electrochemistry: An electrochemical approach to electron transfer chemistry*; John Wiley & Sons, Inc.: Hoboken, NJ, 2006.
(10) Baker-Hawkes, M. J.; Billig, E.; Gray, H. B. *J. Am. Chem. Soc.* **1966**, *88*, 4870−4875.
(11) Bard, A. J.; Faulkner, L. R. *Electrochemical Methods. Fundamentals and Applications*; John Wiley & Sons, Inc.: Hoboken, NJ, 2001.
(12) Kaljurand, I.; Kutt, A.; Soovali, L.; Rodima, T.; Maemets, V.; Leito, I.; Koppel, I. A. *J. Org. Chem.* **2005**, *70*, 1019−1028.
(13) Crabtree, R. H. *Chem. Rev.* **2012**, *112*, 1536−1554.
(14) (a) Dalgleish, S.; Awaga, K.; Robertson, N. *Chem. Commun.* **2011**, *47*, 7089−7091. (b) Dalgleish, S.; Yoshikawa, H.; Matsushita, M. M.; Awaga, K.; Robertson, N. *Chem. Sci.* **2011**, *2*, 316−320.
(15) McNamara, W. R.; Han, Z.; Alperin, P. J.; Brennessel, W. W.; Holland, P. L.; Eisenberg, R. *J. Am. Chem. Soc.* **2011**, *133*, 15368−15371.
(16) Han, Z.; McNamara, W. R.; Eum, M.-S.; Holland, P. L.; Eisenberg, R. *Angew. Chem., Int. Ed.* **2012**, *51*, 1667−1670.
(17) Han, Z.; Qiu, F.; Eisenberg, R.; Holland, P. L.; Krauss, T. D. *Science* **2012**, *338*, 1321−1324.

(18) (a) Begum, A.; Moula, G.; Sarkar, S. *Chem.—Eur. J.* **2010**, *16*, 12324−12327. (b) Begum, A.; Sarkar, S. *Eur. J. Inorg. Chem.* **2012**, *2012*, 40−43.
(19) (a) Capon, J.-F.; Gloaguen, F.; Schollhammer, P.; Talarmin, J. *J. Electroanal. Chem.* **2006**, *595*, 47−52. (b) Capon, J.-F.; Gloaguen, F.; Schollhammer, P.; Talarmin, J. *J. Electroanal. Chem.* **2004**, *566*, 241−247. (c) Sellmann, D.; Geck, M.; Moll, M. *J. Am. Chem. Soc.* **1991**, *113*, 5259−5264.
(20) Liu, Y.-C.; Chu, K.-T.; Jhang, R.-L.; Lee, G.-H.; Chiang, M.-H. *Chem. Commun.* **2013**, *49*, 4743−4745.
(21) (a) Carroll, M. E.; Barton, B. E.; Gray, D. L.; Mack, A. E.; Rauchfuss, T. B. *Inorg. Chem.* **2011**, *50*, 9554−9563. (b) Schilter, D.; Nilges, M. J.; Chakrabarti, M.; Lindahl, P. A.; Rauchfuss, T. B.; Stein, M. *Inorg. Chem.* **2012**, *51*, 2338−2348. (c) Barton, B. E.; Rauchfuss, T. B. *J. Am. Chem. Soc.* **2010**, *132*, 14877−14885. (d) Barton, B. E.; Whaley, C. M.; Rauchfuss, T. B.; Gray, D. L. *J. Am. Chem. Soc.* **2009**, *131*, 6942−6943.
(22) Hunter, C. A.; Sanders, J. K. M. *J. Am. Chem. Soc.* **1990**, *112*, 5525−5534.
(23) McCreery, R. L. *Chem. Rev.* **2008**, *108*, 2646−2687.
(24) Palys, B. J.; Puppels, G. J.; van den Ham, D.; Feil, D. *J. Electroanal. Chem.* **1992**, *326*, 105−112.
(25) (a) Curtis, M. D.; Druker, S. H. *J. Am. Chem. Soc.* **1997**, *119*, 1027−1036. (b) Torres-Nieto, J.; Brennessel, W. W.; Jones, W. D.; García, J. J. *J. Am. Chem. Soc.* **2009**, *131*, 4120−4126. (c) Schaub, T.; Backes, M.; Radius, U. *Chem. Commun.* **2007**, 2037−2039.
(26) Cha, M.; Shoner, S. C.; Kovacs, J. A. *Inorg. Chem.* **1993**, *32*, 1860−1863.
(27) Kambe, T.; Sakamoto, R.; Hoshiko, K.; Takada, K.; Miyachi, M.; Ryu, J.-H.; Sasaki, S.; Kim, J.; Nakazato, K.; Takata, M.; Nishihara, H. *J. Am. Chem. Soc.* **2013**, *135*, 2462−2465.
(28) Loglio, F.; Innocenti, M.; Jarek, A.; Caporali, S.; Pasquini, I.; Foresti, M. L. *J. Electroanal. Chem.* **2010**, *638*, 15−20.
(29) Shalvoy, R. B.; Reucroft, P. J. *J. Vac. Sci. Technol. (N.Y., NY, U.S.)* **1979**, *16*, 567−569.
(30) (a) Selvam, P.; Viswanathan, B.; Srinivasan, V. *J. Electron Spectrosc. Relat. Phenom.* **1989**, *49*, 203−211. (b) Lian, K. K.; Kirk, D. W.; Thorpe, S. J. *J. Electrochem. Soc.* **1995**, *142*, 3704−3712.
(31) Grosvenor, A. P.; Biesinger, M. C.; Smart, R. S. C.; McIntyre, N. S. *Surf. Sci.* **2006**, *600*, 1771−1779.
(32) Hall, D. S.; Bock, C.; MacDougall, B. R. *J. Electrochem. Soc.* **2013**, *160*, F235−F243.
(33) Mi, L.; Ding, Q.; Chen, W.; Zhao, L.; Hou, H.; Liu, C.; Shen, C.; Zheng, Z. *Dalton Trans.* **2013**, *42*, 5724−5730.
(34) Liebeskind, L. S.; Srogl, J.; Savarin, C.; Polanco, C. *Pure Appl. Chem.* **2002**, *74*, 115−122.
(35) Borucinsky, T.; Rausch, S.; Wendt, H. *J. Appl. Electrochem.* **1997**, *27*, 762−773.
(36) (a) Wiebelhaus, N. J.; Cranswick, M. A.; Klein, E. L.; Lockett, L. T.; Lichtenberger, D. L.; Enemark, J. H. *Inorg. Chem.* **2011**, *50*, 11021−11031. (b) Eisenberg, R.; Gray, H. B. *Inorg. Chem.* **2011**, *50*, 9741−9751.
(37) Lipshutz, B. H.; Frieman, B.; Birkedal, H. *Org. Lett.* **2004**, *6*, 2305−2308.
(38) Fry, A. J. In *Laboratory Techniques in Electroanalytical Chemistry*, 2nd ed.; Kissinger, P. T., Heineman, W. R., Eds.; Marcel Dekker, Inc.: New York, 1996; pp 469−483.
(39) Hathaway, B. J.; Holah, D. G.; Underhill, A. E. *J. Chem. Soc.* **1962**, 2444−2448.
(40) Robertson, N.; Parsons, S.; Awaga, K.; Fujita, W. *CrystEngComm* **2000**, *2*, 121−124.